Predicted lithium oxide compounds and superconducting low-pressure LiO_4

Xiao Dong,[1] Jingyu Hou,[1] Jun Kong,[1] Haixu Cui,[2,*] Yan-Ling Li,[3,†] Artem R. Oganov,[4,5,6] Kuo Li,[7] Haiyan Zheng,[7] Xiang-Feng Zhou,[1,8,‡] and Hui-Tian Wang[1,9]

[1]*Key Laboratory of Weak-Light Nonlinear Photonics and School of Physics, Nankai University, Tianjin 300071, China*
[2]*College of Physics and Materials Science, Tianjin Normal University, Tianjin 300387, China*
[3]*Laboratory for Quantum Design of Functional Materials, School of Physics and Electronic Engineering, Jiangsu Normal University, Xuzhou 221116, China*
[4]*Skolkovo Institute of Science and Technology, Skolkovo Innovation Center, 3 Nobel St., Moscow 121205, Russia*
[5]*Moscow Institute of Physics and Technology, 9 Institutskiy Lane, Dolgoprudny city, Moscow Region, 141700, Russia*
[6]*International Center for Materials Discovery, Northwestern Polytechnical University, Xi'an, 710072, China*
[7]*Center for High Pressure Science and Technology Advanced Research, Beijing 100193, China*
[8]*Center for High Pressure Science, State Key Laboratory of Metastable Materials Science and Technology, School of Science, Yanshan University, Qinhuangdao 066004, China*
[9]*National Laboratory of Solid State Microstructures and Collaborative Innovation Center of Advanced Microstructures, Nanjing University, Nanjing 210093, China*

(Received 20 May 2016; revised manuscript received 29 August 2019; published 14 October 2019)

We study the stability of Li-O compounds as a function of pressure, with rich phase diagram, diverse properties, and fundamental chemical interest in mind. Using the *ab initio* evolutionary algorithm USPEX, we predict the stability of compounds LiO_4, Li_5O_3, and Li_6O under pressure. Unexpectedly, LiO_2 will decompose to $Li_2O_2 + LiO_4$ in the pressure range 6–18 GPa. LiO_4, formed at the pressure of just 6 GPa, can be seen as ε-O_8 accepting two electrons from two Li atoms. This phase is superconducting, with T_c up to 12.2 K at 10 GPa. This is remarkable, because elemental oxygen becomes superconducting at much higher pressure (96 GPa) and has much lower T_c (<0.6 K), and suggests that chemical alloying with other elements has the potential of not only decreasing metallization pressure, but also of increasing T_c. Since ε-O_8 is called red oxygen, LiO_4 can be identified as "lithium red-oxide", and is distinct from superoxide. Additionally, Li_5O_3 is stable at pressures above 70 GPa and can be represented as a hybrid structure $4Li_2O \cdot Li_2O_2$, and electride suboxide Li_6O is stable above 62 GPa.

DOI: 10.1103/PhysRevB.100.144104

I. INTRODUCTION

Oxygen is one of the most abundant and important elements. However, elemental oxygen is unique in many ways: at zero pressure, it is the only known elemental molecular magnet with a triplet state as its ground state. The O_2 molecule has half-filled $2\pi^*_{p_x}$ and $2\pi^*_{p_y}$ orbitals. At high pressure, the O_2 molecules cluster together, forming a nonmagnetic ε phase with O_8 clusters [1–3]. It is believed that unpaired bonding orbitals of the neighboring O_2 dimers overlap, which induces electron pairing and formation of intermolecular bonds. At higher pressure, metallization is observed around 100 GPa upon the formation of ζ-O_2, which is confirmed to have superconductivity at temperatures below 0.6 K [4].

At atmospheric pressure, alkali metals are thought to be the most electropositive elements. They adopt the +1 oxidation state and form ionic crystals with electronegative elements. Together with oxygen molecule, they react exothermically and usually form oxides, peroxides or superoxides; heavy alkalis (K, Rb, Cs) are also known to form suboxides (such as Rb_6O and Rb_9O_2). Specifically, the superoxide anion has one unpaired electron and behaves as a free radical. At low temperatures, superoxides are calculated to be ferromagnetic (FM) or antiferromagnetic (AFM) [5,6] and have some characteristics more typical of compounds of d-block and f-block elements: for example, RbO_2 is thought to be a Mott insulator [7]. However, compared with d-block elements, the localized unpaired electrons in superoxides have a weak exchange effect, so their Curie temperatures are low and there is usually a paramagnetic state at room temperature. Both the oxygen molecule O_2 and the superoxide ion O_2^- undergo spin pairing and lose magnetism under pressure. More interestingly, unlike semiconducting cluster phase ε-O_2, by doping with electrons, superoxide ion goes directly to the metallic state, but without observable superconductivity.

Lithium is the smallest alkali metal atom, and its oxide plays an important role in the lithium-air battery. The known oxides are Li_2O and Li_2O_2. Some also consider LiO_2 to exist in the gas phase [8,9], e.g. in the discharge media of Li-O_2 battery [10] or on specific substrates, such as graphene [11]. However, pure LiO_2 crystals have hardly ever been obtained at normal conditions, because LiO_2 is thermodynamically unstable with respect to disproportionation, giving Li_2O_2 [11–13].

*Corresponding author: hxcui@tjnu.edu.cn
†ylli@jsnu.edu.cn
‡xfzhou@nankai.edu.cn; zxf888@163.com

A theoretical structure prediction study [14] also reported Li_3O_4 to be stable as a hybrid structure of $Li_2O_2 \cdot LiO_2$.

Recent theoretical and experimental investigations found that pressure greatly affects chemical properties of the elements. For example, pressure increases the reactivity of xenon and its oxides become thermodynamically stable at moderate and experimentally reachable pressure (>83 GPa) [15]. Caesium becomes a *p*-block element and the formation of $CsF_n (n > 1)$ compounds was predicted [16,17]. Sodium becomes an extremely electropositive element and forms a very stable compound Na_2He with the normally inert element He at pressures above ~120 GPa [18]. Furthermore, under pressure, unexpected sodium chlorides, such as Na_3Cl and $NaCl_3$, become stable [19].

II. METHODS

Since oxygen and superoxide ion lose their magnetism and their state changes with increasing pressure, we expected that there will be different chemical behaviors in the Li-O system at high pressure. Here we performed structure prediction with a variable-composition evolutionary algorithm [20], as implemented in the USPEX code [21]. In such calculations, a phase is deemed stable if its enthalpy of formation from the elements or any other possible compounds is negative. A number of applications [15,19,21–23] illustrate its power. Variable-composition structure searches with spin polarization were performed for the Li-O system at pressures of 0, 10, 20, 50, 70, and 100 GPa, allowing up to 45 atoms per primitive cell. Structure relaxations were performed using density functional theory within the Perdew-Burke-Ernzerhof (PBE) functional [24] in the framework of the all-electron projector augmented wave (PAW) method [25] as implemented in the VASP code [26]. For Li atoms, we used PAW potentials with 1.2 a.u. core radius and $1s^2 2s$ electrons treated as valence; for O the core radius was 1.15 a.u. and $2s^2 2p$ [4] electrons were treated as valence. We used a plane-wave kinetic energy cutoff of 1000 eV, and the Brillouin zone was sampled by a *k*-points mesh with a reciprocal-space resolution of $2\pi \times 0.03$ Å^{-1}, which showed excellent convergence of the energy differences, stress tensors, and structural parameters. The Heyd–Scuseria–Ernzerhof (HSE) hybrid functional [27] was used to examine the metallization and semiconductivity of the Li-O compounds. Phonon calculations were performed for all promising structures using the PHONOPY code [28]. Electron-phonon coupling and superconductivity calculations were performed using the Quantum Espresso package [29] with a $6 \times 6 \times 6$ *q* grid for a primitive cell of LiO_4.

III. RESULTS AND DISCUSSIONS

Unexpectedly, we found a series of compounds, such as LiO_4, Li_5O_3, Li_6O, which have lower enthalpy than the mixture of elemental Li and O, or any other mixture at pressures below 100 GPa. Their structures are listed in Table I. In our calculations, the ordinary ambient-pressure phases, *Pnnm* LiO_2, $P6_3/mmc$ Li_2O_2, and Fm-$3m$ Li_2O are successfully reproduced and their crystal structures are consistent with previous experimental and theoretical works [10,12,14,30–35]. For other theoretically predicted phases, such as P-$6m2$ Li_3O_4, our calculations (taking great care for the precision and quality of the PAW potential) indicate metastabilty.

LiO_2 is found to undergo a phase transition from *Pnnm* to $P4/mbm$ at the pressure of 12 GPa (Fig. 1), and this transition is a direct analog of the NaCl-CsCl structural transition (if one treats the superoxide group O_2^- as a single particle), well known in binary ionic systems at high pressure. In the *Pnnm* phase, Li is inside the oxygen layer and has shorter distance (2.35 Å at 10 GPa) to superoxide anion than in $P4/mbm$ (2.49 Å at 10 GPa), making it easier to bridge the localized spin densities by a superexchange interaction, as reported in alkali metal superoxides [5–7]. Thus, this phase has a nonzero magnetic moment in its ground state. When the O_2^- groups are forced closer by pressure, the superexchange interaction competes with spin pairing tendency, which triggers a magnetic transition from high spin state ($1\mu_B$ per O_2^-) to low spin state (nearly $0.2\mu_B$ per O_2^-) at 6 GPa. The *Pnnm* phase remains weakly magnetic until the net spin decreases to zero at 35 GPa. In the $P4/mbm$ structure, Li and O are in different layers, so Li is far away and unable

TABLE I. Structures of $P4/mbm$-LiO_2, $I4/mcm$-LiO_4, P-6 $2m$-Li_6O and $I4/m$ Li_5O_3

Stoichiometry	Space group (No.)	Pressure	Lattice parameters	Atomic positions
LiO_2	$P4/mbm$ (127)	10 GPa	$a = b = 4.35$ Å $c = 2.42$ Å $\alpha = \beta = \gamma = 90^\circ$	Li 2*a* (0,0,0) O 4*h* (0.108,0.608,0.5)
LiO_4	$I4/mcm$ (140)	10 GPa	$a = b = 4.73$ Å $c = 7.35$ Å $\alpha = \beta = \gamma = 90^\circ$	Li 4*a* (0, 0, 0.25) O 16l (0.195, 0.305,0.414)
Li_6O	P-6 $2m$ (189)	80 GPa	$a = b = 4.18$ Å $c = 2.74$ Å $\alpha = \beta = 90^\circ$, $\gamma = 120^\circ$	Li 3*f* (0.726,0,0) Li 3*g* (0.418,0,0.5) O 1*b* (0, 0, 0.5)
Li_5O_3	$I4/m$ (87)	80 GPa	$a = b = 6.86$ Å $c = 3.40$ Å $\alpha = \beta = \gamma = 90^\circ$	Li 4*d* (0,0.5,0.25) Li 8*h* (0.414,0.286,0) Li 8*h* (0.227,0.092,0) O 4*e* (0,0,0.210) O 8*h* (0.653, 0.153, 0)

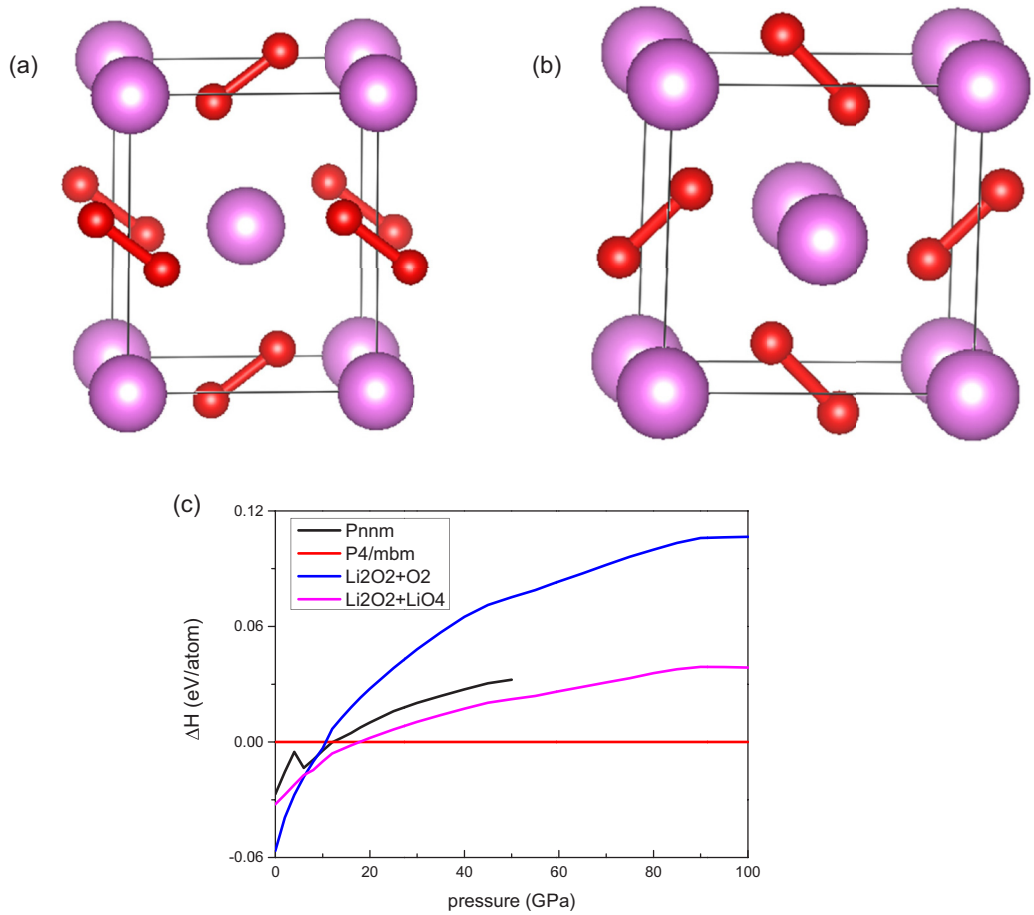

FIG. 1. Structures of LiO_2. (a) *Pnnm*, (b) $P4/mbm$. (c) Enthalpies relative to $P4/mbm$ LiO_2 as a function of pressure. The discontinuous curve of the *Pnnm* phase means a spontaneous phase transition from high spin to low spin.

to bridge the unpaired spin densities of O_2^- groups, and this phase loses its magnetism at a low pressure of 2 GPa. This phase with eight-fold coordination is denser and the corresponding reduction of the PV-term renders it more stable at high pressure. Thus, in addition to the growth of LiO_2 on graphene substrate [11], crystalline LiO_2 can be made under pressure. Our investigation of thermodynamic stability shows that at atmospheric pressure, LiO_2 is metastable, and decomposition into $Li_2O_2 + O_2$ (0–6 GPa) or $Li_2O_2 + LiO_4$ (6–18 GPa) is favorable. This decomposition at zero pressure is consistent with previous calculations [12,13] and with the known problems of obtaining pure crystalline LiO_2. Only at pressures above 18 GPa does LiO_2 become stable.

Furthermore, the compound LiO_4 is calculated to become thermodynamically stable at a remarkably low pressure of 6 GPa, and the following reactions,

$$Li_2O_2 + 2O_2 \rightarrow 2LiO_4, \quad (1)$$

$$3LiO_2 \rightarrow Li_2O_2 + LiO_4, \quad (2)$$

are both predicted to be exothermic at pressures between 6 and 18 GPa. Above 18 GPa, LiO_2 and LiO_4 coexist up to at least 100 GPa. Phonon calculations [Fig. 3(e)] clearly indicate dynamical stability of LiO_4 from 0 to 100 GPa, which means once formed at high pressure, this phase can be quenchable to ambient conditions.

As shown in Fig. 2(c), LiO_4 has only one ground-state structure from 6 to at least 100 GPa, and this structure [shown in Figs. 3(a) and 3(b)] has a body-centered tetragonal space group $I4/mcm$. At 10 GPa, O atoms occupy the Wyckoff position 16l (0.195, 0.305, 0.414), Li atoms occupy the 4*a* (0, 0, 0.25) positions and the lattice parameters are $a = b = 4.73$ Å, $c = 7.35$ Å. This structure consists of layers of oxygen dimers alternating with Li layers. Particularly, in one conventional cell, the oxygen layer is made of four oxygen dimers forming an O_8 cluster, which looks like a square when viewed along the O_2 molecules. The squares in different layers do not align and have a rotation, for example, 25° at 10 GPa. That is why the structure of LiO_4 is seen as a flower with eight petals in its [001] direction [Fig. 3(b)]. The O-O distance in LiO_4 (1.26 Å at 10 GPa) lies in between that in the neutral oxygen molecule (1.21 Å at 10 GPa) and in the superoxide anion O_2^- (1.32 Å at 10 GPa), which implies an intermediate bonding situation. The band structure shows LiO_4 to be a two-dimensional metal, with conductivity along the oxygen layer [Fig. 3(c)]. The Fermi level of LiO_4 goes through the O-Oπ^* band, like in LiO_2. Both LiO_4 and LiO_2 are typical *p*-type conductors, which can be seen as the saturated system Li_2O_2 doped with oxygen dimers. The π^* band in $P4/mbm$ LiO_2 is broader than in LiO_4.

As shown in Fig. 3(e), the calculated phonon spectrum proves the dynamical stability in the pressure range from 0

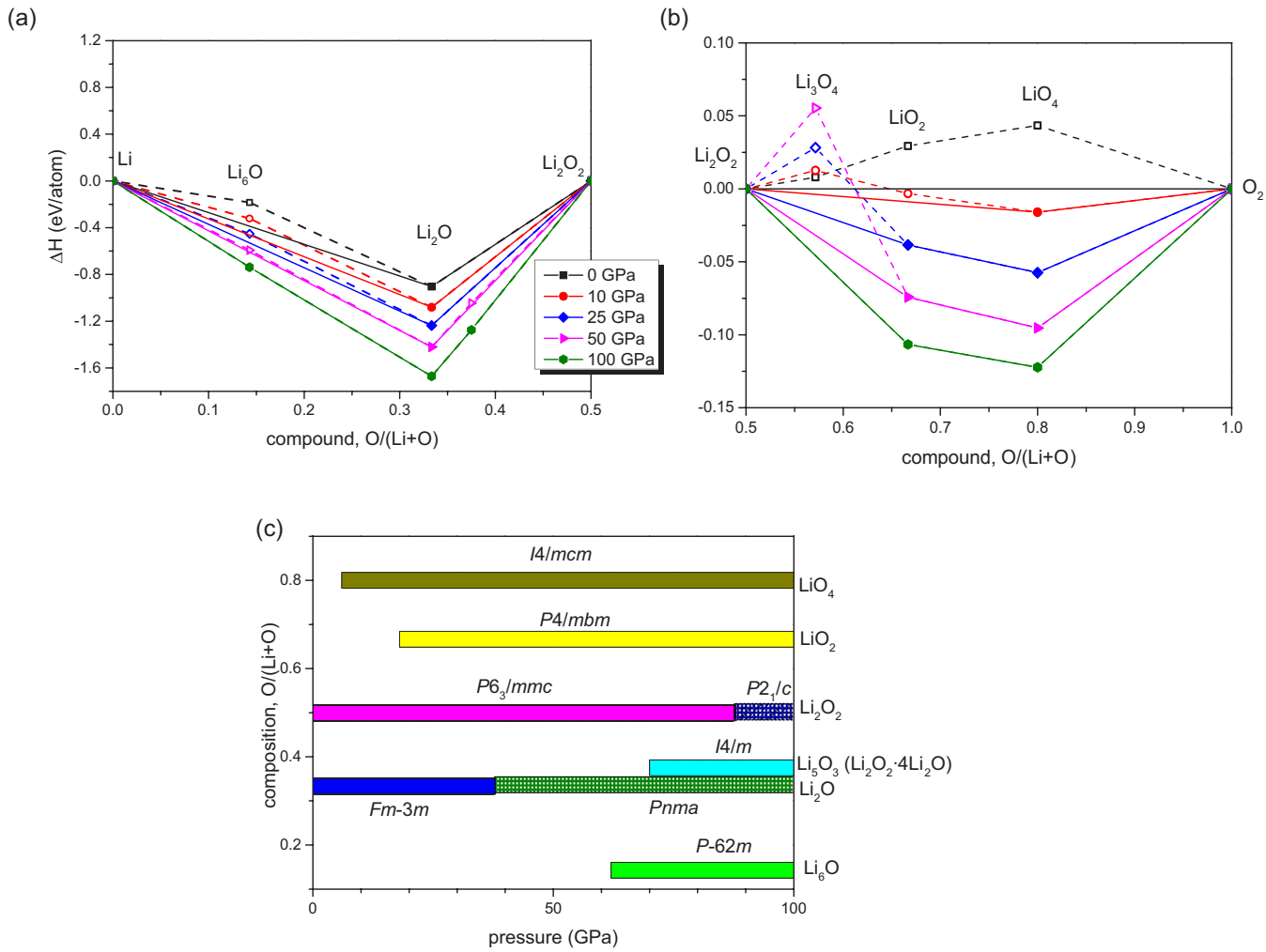

FIG. 2. Thermodynamics of the Li-O system: (a), (b) Predicted convex hulls of the Li-O system at 0, 10, 25, 50, and 100 GPa. For clarity, we show separately (a) Li-rich and (b) O-rich parts of the system. In (c), we show the pressure-composition phase diagram of the Li-O system.

to 100 GPa. There is a wide phonon gap up to 20.2 THz at zero pressure in its phonon spectrum, suggesting that LiO_4 is a quasimolecular system with its oxygen dimers. At 10 GPa, frequencies of Raman-active oxygen stretching vibrations are 43.5 (B_{2g}) and 37.0 THz (A_{1g}), which are intermediate between elemental oxygen O_2 (48.0 THz) and *Pnnm* LiO_2 (37.0 and 33.1 THz). So LiO_4 can be identified by Raman frequency in the experiments.

The formation of lithium superoxide LiO_2 at high pressure is consistent with the existence at ambient pressure of such alkali metal superoxides as NaO_2, KO_2, RbO_2, and CsO_2. However, LiO_4 was never reported, has no known analogs and is unexpected from classical chemical rules. We can draw, however, some analogies with high-pressure phases ε-O_8 [1–3] and $NaCl_3$ [19]: The former has a structural relationship to LiO_4 and the latter has an electronic similarity with it (it is a metal due to the anion sublattice, just like LiO_4). LiO_4 can be seen as ε-O_8 accepting two electrons from Li atoms.

Molecular oxygen, with half-filled π^* bands, should be metallic, but a band gap opens through magnetization (Stoner mechanism) and distortion (Peierls mechanism) to lower the energy. In semiconducting ε-O_8, there are two kinds of intermolecular distances, 2.12 and 2.72 Å at 10 GPa, within and between the O_8 clusters. Under pressure, magnetism is suppressed and Peierls distortion vanishes because of its increased elastic energy cost and unfavorable volume increase, and this leads to metallization of oxygen at 96 GPa. Injecting the Peierls-unstable metallic system with electrons can widen its stability field and make it stable at lower pressures, as we see in $NaCl_3$ (Peierls distortion disappears at 48 GPa, compared to ~160 GPa in Cl_2) and in LiO_4 (metallization and disappearance of the Peierls distortion at just 6 GPa, compared to 96 GPa in pure oxygen). At 10 GPa, the O-O distance between oxygen dimers is 2.42 Å, just similar to the average distance in ε-O_8.

Inhibition of the Peierls transition usually means high electron-phonon coupling, which leads to superconductivity; for example, ζ-O_2 is a superconductor with critical temperature $T_c = 0.6$ K at 100 GPa [4]. High density of states (DOS) at the Fermi level and high vibrational frequencies are the other factors raising T_c in Bardeen-Cooper-Schrieffer theory [36]. Using the Allen-Dynes modified McMillan equation [37] with the commonly accepted value of the Coulomb pseudopotential $\mu^* = 0.1$, for LiO_4 we obtained T_c up to 12 K at 10 GPa, decreasing with pressure to 0.5 K at 100 GPa (Fig. 4),

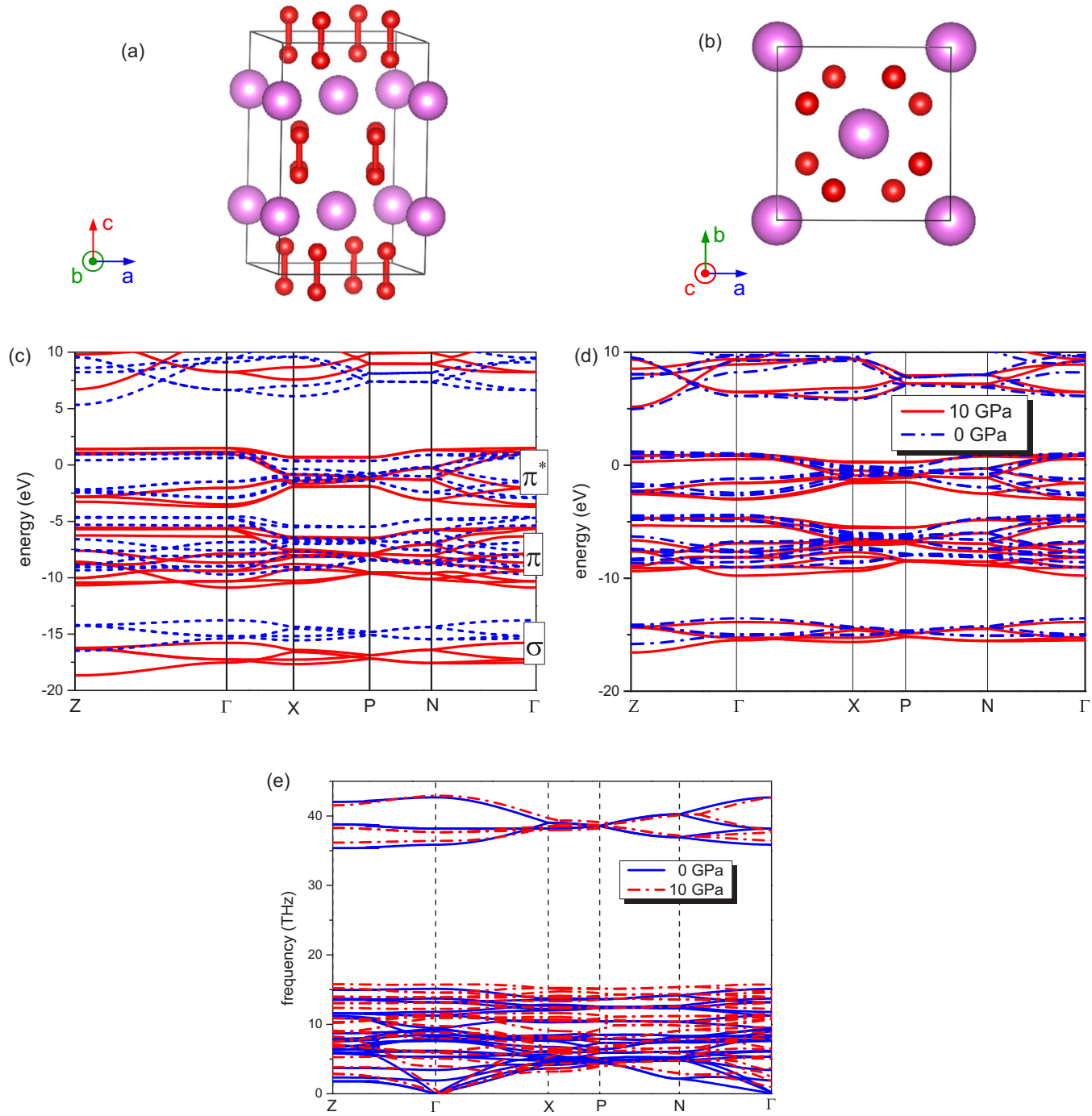

FIG. 3. Conventional cell of LiO_4 in (a) [010] and (b) [001] directions. (c) Band structure of LiO_4 at 10 GPa. The red solid lines are calculated with HSE hybrid functional and the blue dotted lines are from the PBE functional. Bands formed by $2p$ electrons are indicated. Fermi level is set to zero. (d) Evolution of the band structure from 0 to 10 GPa (computed using PBE functional). (e) Phonon spectrum of LiO_4 at 0 and 10 GPa.

which is quite near the T_c of metallic oxygen molecular at 100 GPa. The DOS at Fermi level of LiO_4 decreases sharply with pressure, which implies the metallicity is inhibited and T_c falls down with pressure (Fig. 4).

Doping by highly electropositive atoms, which donate their electrons to nonmetal atoms and can increase the DOS at the Fermi level, can lead to high-T_c superconductors (for example, CaC_6 [38,39]). Here, by adding lithium we not only decrease the pressure of onset of superconductivity to just 6 GPa, but also increase T_c to 12 K (which coincides with the T_c of CaC_6).

Since ε-O_8 is called red oxygen, LiO_4 can be called "lithium red-oxide" to emphasize its relationship with ε-O_8 and distinguish it from superoxide. Metallic and superconducting, LiO_4 has a low formation pressure and is predicted to remain dynamically stable at 0 GPa. Since metastable phase LiO_2 can grow on specific substrate [11], LiO_4 can also be

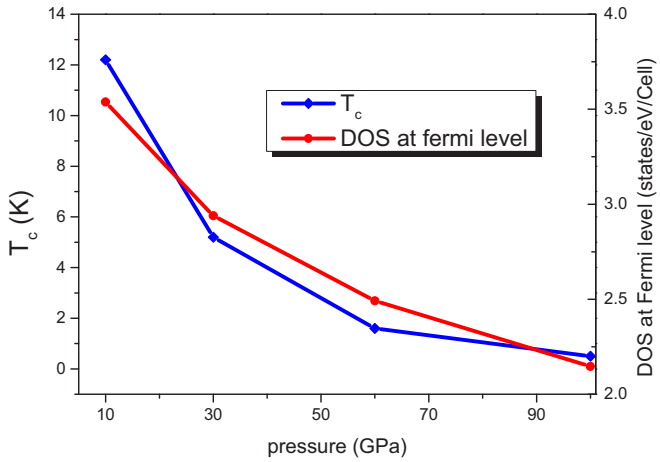

FIG. 4. Critical temperature of superconductivity (T_c) and DOS at the Fermi level as a function of pressure.

stabilized on properly chosen substrates and might find use in lithium batteries.

Upon further increase of pressure, two compounds become thermodynamically stable: Li_5O_3 at 70 GPa and Li_6O at 62 GPa [Fig. 2(c)]. Li_5O_3 can be written as $4Li_2O \cdot Li_2O_2$, as shown in Fig. 5(b); this is a peroxide-oxide compound with simultaneous presence of oxide and peroxide ions at high pressure (such compounds become stable in the Al-O system at pressures above 300 GPa [40]).

Li_6O is a suboxide. Like pure Li [41–44], Li_6O at high pressure is an electride with a 1:2 ratio of O ions and localized electron pairs, so the true formula is $Li_6O(2e)_2$. As shown in Fig. 5(a), every oxygen and localized electron pair are surrounded by a Li polyhedron of nine vertexes, 21 edges, and 14 triangular faces. A similar electride suboxide, Mg_3O_2, was also reported [45] at high pressure. Li_6O is a nonsuperconducting metal.

We noticed an experimental work [46] to synthesize mixtures of a series of lithium oxides at high pressure. They reported phases of Li_2O_2, LiO_2 similar to our result and LiO_4 with space group of *Ibam*, which is a subgroup of our *I4/mcm*. However, in a more accurate calculation, *Ibam*-LiO_4 relaxes directly to *I4/mcm*. The experimental observation of *Ibam* needs to be checked by further experiments. In addition, the

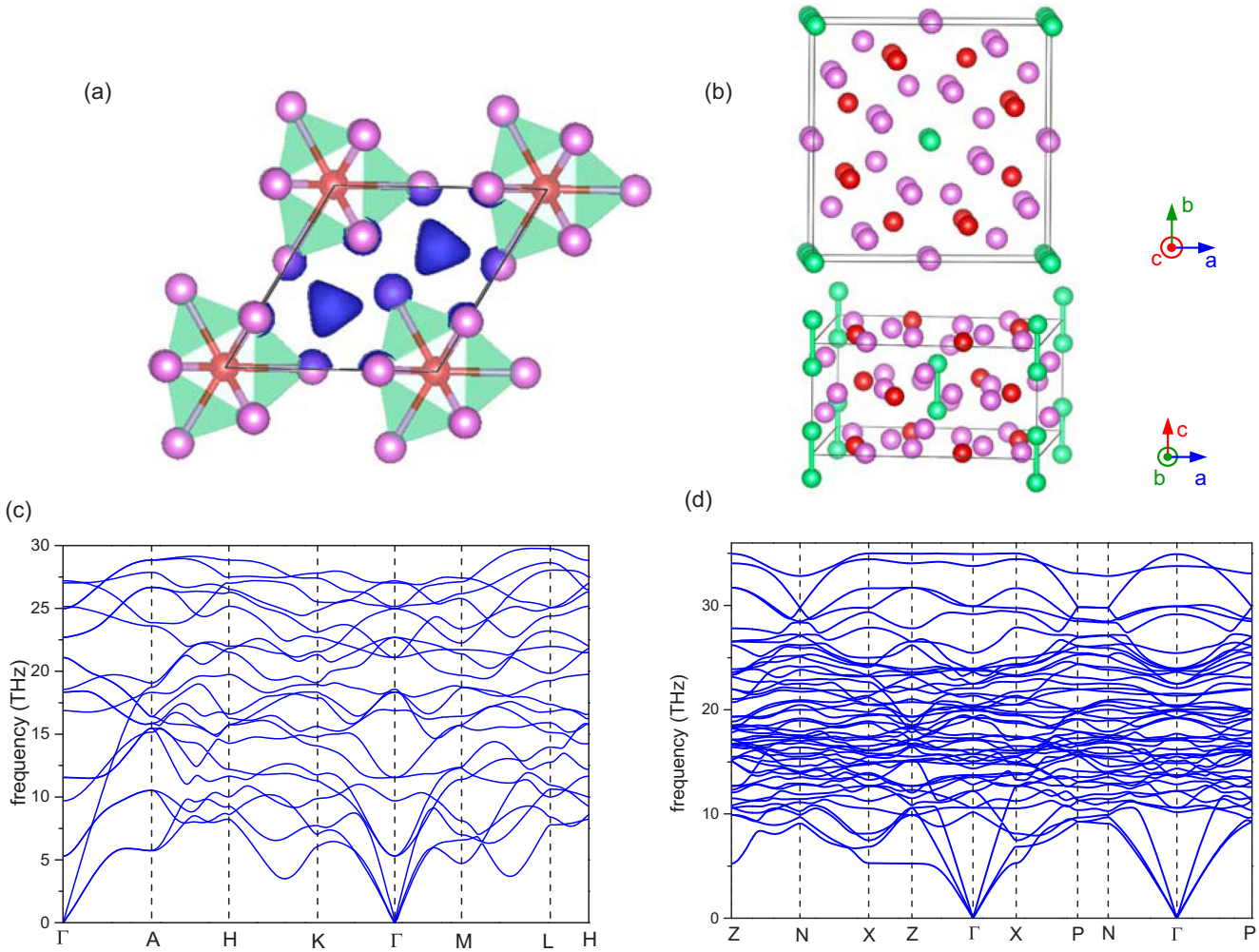

FIG. 5. Crystal structures of (a) Li_6O and (b) Li_5O_3 and their phonon spectra at 80 GPa [(c) and (d), respectively]. In (a) we also show a green isosurface with ELF = 0.9. In (b), the structure is shown in the [010] and [001] directions with peroxide ions colored green and the oxide ion colored red.

experiment showed that mixture of Li_2O_2 with oxygen cannot get a pure phase. More controllable conditions such as temperatures and synthesis methods are necessary for synthesis of pure LiO_2 or LiO_4.

In conclusion, a systematic search for stable compounds yielded three lithium oxides, LiO_4, Li_5O_3, Li_6O. Of particular interest is LiO_4, which becomes stable at just 6 GPa and can be seen as ε-O_8 doped with two electrons from two lithium atoms. This phase is dynamically stable at atmospheric pressure. With Li injecting its electrons to greatly increase conductivity, LiO_4 has electronic conduction within the oxygen layers and superconducting $T_c = 12$ K, much higher than that of pure oxygen, 0.6 K. After 10 GPa, T_c decreases with the pressure, due to decreasing density of states at the Fermi level for LiO_4. These compounds not only display unusual chemistry, but also might play a role in Li batteries.

ACKNOWLEDGMENTS

This work was supported by NSFC (Grants No. 21803033, No. 11674176, No. 11874224, No. 21771011, No. 11674131, and No. 11604290) and Yong Elite Scientists Sponsorship Program by Tianjin (Grant No. TJSQNTJ-2018-18). The work of A. R. O. was supported by Russian Science Foundation (Grant No. 19-72-30043). The calculations were performed at Tianhe II in Guangzhou.

[1] H. Fujihisa, Y. Akahama, H. Kawamura, Y. Ohishi, O. Shimomura, H. Yamawaki, M. Sakashita, Y. Gotoh, S. Takeya, and K. Honda, Phys. Rev. Lett. **97**, 085503 (2006).
[2] L. F. Lundegaard, G. Weck, M. I. Mcmahon, S. Desgreniers, and P. Loubeyre, Nature (London) **443**, 201 (2006).
[3] Y. Meng, P. J. Eng, J. S. Tse, D. M. Shaw, M. Y. Hu, J. Shu, S. A. Gramsch, C. Kao, R. J. Hemley, and H.-K. Mao, Proc. Natl. Acad. Sci. USA **105**, 11640 (2008).
[4] K. Shimizu, K. Suhara, M. Ikumo, M. I. Eremets, and K. Amaya, Nature (London) **393**, 767 (1998).
[5] S. D. Mahanti and A. U. Khan, Solid State Commun. **18**, 159 (1976).
[6] H. G. Smith, R. M. Nicklow, L. J. Raubenheimer, and M. K. Wilkinson, J. Appl. Phys. **37**, 1047 (1966).
[7] R. Kováčik, P. Werner, K. Dymkowski, and C. Ederer, Phys. Rev. B **86**, 075130 (2012).
[8] L. Andrews, J. Chem. Phys. **50**, 4288 (1969).
[9] V. S. Bryantsev, M. Blanco, and F. Faglioni, J. Phys. Chem. A **114**, 8165 (2010).
[10] J. Yang, D. Zhai, H.-H. Wang, K. C. Lau, J. A. Schlueter, P. Du, D. J. Myers, Y.-K. Sun, L. A. Curtiss, and K. Amine, Phys. Chem. Chem. Phys. **15**, 3764 (2013).
[11] J. Lu, Y. Jung Lee, X. Luo, K. Chun Lau, M. Asadi, H.-H. Wang, S. Brombosz, J. Wen, D. Zhai, Z. Chen, D. J. Miller, Y. Sub Jeong, J.-B. Park, Z. Zak Fang, B. Kumar, A. Salehi-Khojin, Y.-K. Sun, L. A. Curtiss, and K. Amine, Nature (London) **529**, 377 (2016).
[12] S. Kang, Y. Mo, S. P. Ong, and G. Ceder, Chem. Mater. **25**, 3328 (2013).
[13] M. M. Islam and T. Bredow, J. Phys. Chem. C **113**, 672 (2009).
[14] G. Yang, Y. Wang, and Y. Ma, J. Phys. Chem. Lett. **5**, 2516 (2014).
[15] Q. Zhu, D. Y. Jung, A. R. Oganov, C. W. Glass, C. Gatti, and A. O. Lyakhov, Nat. Chem. **5**, 61 (2013).
[16] M. S. Miao, Nat. Chem. **5**, 846 (2013).
[17] Q. Zhu, A. R. Oganov, and Q. Zeng, Sci. Rep. **5**, 7875 (2015).
[18] X. Dong, A. R. Oganov, A. F. Goncharov, E. Stavrou, S. Lobanov, G. Saleh, G.-R. Qian, Q. Zhu, C. Gatti, V. L. Deringer, R. Dronskowski, X.-F. Zhou, V. B. Prakapenka, Z. Konôpková, I. A. Popov, A. I. Boldyrev, and H.-T. Wang, Nat. Chem. **9**, 440 (2017).
[19] W. Zhang, A. R. Oganov, A. F. Goncharov, Q. Zhu, S. E. Boulfelfel, A. O. Lyakhov, E. Stavrou, M. Somayazulu, V. B. Prakapenka, and Z. Konôpková, Science **342**, 1502 (2013).
[20] A. O. Lyakhov, A. R. Oganov, and M. Valle, *Modern Methods of Crystal Structure Prediction*, edited by A. R. Oganov (Wiley-VCH, Germany, 2010), p. 147.
[21] A. R. Oganov and C. W. Glass, J. Chem. Phys. **124**, 244704 (2006).
[22] Y. Ma, M. Eremets, A. R. Oganov, Y. Xie, I. Trojan, S. Medvedev, A. O. Lyakhov, M. Valle, and V. Prakapenka, Nature (London) **458**, 182 (2009).
[23] A. R. Oganov, J. Chen, C. Gatti, Y. Ma, Y. Ma, C. W. Glass, Z. Liu, T. Yu, O. O. Kurakevych, and V. L. Solozhenko, Nature (London) **457**, 863 (2009).
[24] J. P. Perdew, K. Burke, and M. Ernzerhof, Phys. Rev. Lett. **77**, 3865 (1996).
[25] P. E. Blochl, Phys. Rev. B **50**, 17953 (1994).
[26] G. Kresse and J. Furthmuller, Comput. Mater. Sci. **6**, 15 (1996).
[27] J. Heyd, G. E. Scuseria, and M. Ernzerhof, J. Chem. Phys. **118**, 8207 (2003).
[28] A. Togo, F. Oba, and I. Tanaka, Phys. Rev. B **78**, 134106 (2008).
[29] G. Paolo, B. Stefano, B. Nicola, C. Matteo, C. Roberto, C. Carlo, C. Davide, L. C. Guido, C. Matteo, D. Ismaila, C. Andrea Dal, G. Stefano De, F. Stefano, F. Guido, G. Ralph, G. Uwe, G. Christos, K. Anton, L. Michele, M.-S. Layla, M. Nicola, M. Francesco, M. Riccardo, P. Stefano, P. Alfredo, P. Lorenzo, S. Carlo, S. Sandro, S. Gabriele, P. S. Ari, S. Alexander, U. Paolo, and M. W. Renata, J. Phys.: Condens. Matter **21**, 395502 (2009).
[30] D. U. Tulyaganov, S. Agathopoulos, H. R. Fernandes, and J. M. F. Ferreira, J. Eur. Ceram. Soc. **26**, 1131 (2006).
[31] L. G. Cota and P. De La Mora, Acta Crystallogr. Sect. B **61**, 133 (2005).
[32] M. D. Radin, J. F. Rodriguez, F. Tian, and D. J. Siegel, J. Am. Chem. Soc. **134**, 1093 (2012).
[33] Y. Mo, S. P. Ong, and G. Ceder, Phys. Rev. B **84**, 205446 (2011).
[34] T. Ogasawara, A. Débart, M. Holzapfel, P. Novák, and P. G. Bruce, J. Am. Chem. Soc. **128**, 1390 (2006).
[35] Y.-C. Lu, D. G. Kwabi, K. P. C. Yao, J. R. Harding, J. Zhou, L. Zuin, and Y. Shao-Horn, Energy Environ. Sci. **4**, 2999 (2011).
[36] J. Bardeen, L. N. Cooper, and J. R. Schrieffer, Phys. Rev. **106**, 162 (1957).
[37] P. B. Allen and R. C. Dynes, Phys. Rev. B **12**, 905 (1975).

[38] G. Profeta, M. Calandra, and F. Mauri, Nat. Phys. **8**, 131 (2012).
[39] Y.-L. Li, W. Luo, X.-J. Chen, Z. Zeng, H.-Q. Lin, and R. Ahuja, Sci. Rep. **3**, 3331 (2013).
[40] Y. Liu, A. R. Oganov, S. Wang, Q. Zhu, X. Dong, and G. Kresse, Sci. Rep. **5**, 9518 (2015).
[41] C. J. Pickard and R. J. Needs, Phys. Rev. Lett. **102**, 146401 (2009).
[42] J. Lv, Y. Wang, L. Zhu, and Y. Ma, Phys. Rev. Lett. **106**, 015503 (2011).
[43] M. Marqués, M. I. McMahon, E. Gregoryanz, M. Hanfland, C. L. Guillaume, C. J. Pickard, G. J. Ackland, and R. J. Nelmes, Phys. Rev. Lett. **106**, 095502 (2011).
[44] C. L. Guillaume, E. Gregoryanz, O. Degtyareva, M. I. McMahon, M. Hanfland, S. Evans, M. Guthrie, S. V. Sinogeikin, and H. K. Mao, Nat. Phys. **7**, 211 (2011).
[45] Q. Zhu, A. R. Oganov, and A. O. Lyakhov, Phys. Chem. Chem. Phys. **15**, 7696 (2013).
[46] W. Yang, D. Y. Kim, L. Yang, N. Li, L. Tang, K. Amine, and H.-K. Mao, Adv. Sci. **4**, 1600453 (2017).